Multiple Scattering of EM Waves by Spheres Part I—Multipole Expansion and Ray-Optical Solutions

JOHN H. BRUNING, MEMBER, IEEE, AND YUEN T. LO, FELLOW, IEEE

Abstract—Solution to the multiple scattering of electromagnetic (EM) waves by two arbitrary spheres has been pursued first by the multipole expansion method. Previous attempts at numerical solution have been thwarted by the complexity of the translational addition theorem. A new recursion relation is derived which reduces the computation effort by several orders of magnitude so that a quantitative analysis for spheres as large as 10λ in radius at a spacing as small as two spheres in contact becomes feasible. Simplification and approximation for various cases are also given. With the availability of exact solution, the usefulness of various approximate solutions can be determined quantitatively. For high frequencies, the ray-optical solution is given for two conducting spheres. In addition to the geometric and creeping wave rays pertaining to each sphere alone, there are rays that undergo multiple reflections, multiple creeps, and combinations of both, called the hybrid rays. Numerical results show that the ray-optical solution can be accurate for spheres as small as λ/4 in radius is some cases. Despite some shortcomings, this approach provides much physical insight into the multiple scattering phenomena.

Introduction

THE SIMPLEST realistic problem of multiple scattering by finite bodies appears to be that by two spheres. Many works [1]–[9] on this subject can be found in the literature, but most either deal with general formulation or are confined to specific cases, and practically none give numerical results. Even the limited amount of experimental works by Mevel [2] and Angelakos and Kumagai [5] are in need of independent verification and extension.

It is not the intent of this paper to include a general survey of all the works on this subject, for which the readers are referred to the excellent reviews by Twersky and Burke [10], [11] and also [12]. Here citations will be made only to closely related works.

Manuscript received August 3, 1970. This work was supported in part by NSF under Grant GK4161 and in part by the Bendix Missile System Division under a Research Grant. This paper is based in part on a dissertation submitted by J. H. Bruning in partial fulfillment of the requirements for the Ph.D. degree.

J. H. Bruning was with the Antenna Laboratory, University of Illinois, Urbana, Ill. 61801. He is now with Bell Telephone Laboratories, Murray Hill, N. J. 07971.

Y. T. Lo is with the Antenna Laboratory, University of Illinois, Urbana, Ill. 61801.

In 1935 Trinks [1] considered scattering by two identical spheres of radii much smaller than wavelength, which was later extended to small unequal spheres and arbitrary angle of incidence by Germogenova [4]. More recently Liang and Lo [7] and Crane [9] reformulated the problem using a newly derived translational addition theorem by Stein [13] and Cruzan [14] whereas Twersky [8] considered a more general problem with many scatterers, using dyadic Green's function approach. He also obtained approximate solutions under various conditions.

More recently Levine and Olaofe [15] extended Trinks' work to arbitrary orientation of two small particles and also considered the effect of the electric quadrupole. Even with the help of several previous theoretical works and the availability of modern high speed computers, Liang and Lo [7] found that their numerical evaluation had to be limited to spheres of radii less than 3λ/4 and wide spacings, due to the complexity of the addition theorem. This suggests that the numerical aspect of the problem is by no means trivial.

In this paper the additional theorem as applied to the present problem is reexamined from a numerical point of view. An important recursion relation is introduced which permits a routine calculation of the translation coefficients without resorting to the time-consuming computation of Wigner's 3-j symbols [7]. In doing so, the computing effort can be reduced by several orders of magnitude. As a result, quantitative analyses for spheres as large as 10λ in radius, of arbitrary materials, even in contact become feasible. Closed form approximate solutions under various conditions are also given for the purpose of determining their validity by comparing them with exact ones numerically.

Like all other scattering problems, a multipole expansion solution loses its effectiveness at high frequencies. Therefore, in that case, a ray-optical solution is very desirable. Furthermore, this type of solution offers much physical insight into the complex multiple scattering mechanism. The ray-optical solution is based on the classical geometric optics and creeping wave theory. With the exception of endfire incidence, the numerical results are in excellent agreement with those obtained by multipole expansion for conducting spheres as small as λ/4

in some cases. It is gratifying to see that there exists such a large overlapping region ($\lambda/4$–10λ) between two types of solutions which gives us ample latitude for cross-checks of the results. The confidence on these solutions is further strengthened by observing amazingly close agreement with the experimental results which are discussed in [25].

Statement of Problem and Multipole Expansion Solution

Consider two spheres A and B of arbitrary materials and radii a and b, respectively. Without loss of generality, their centers 0 and 0′, separated by a distance d, can be assumed to lie on the z axis, as shown in Fig. 1. Any point in space can be represented by (r,θ,ϕ) or (r',θ',ϕ) with respect to the coordinate system with origins at 0 or at 0′, which is related to the former through a translation d along the z axis. In the following, we shall adopt the convention that all unprimed quantities are referred to the 0 system whereas all primed are referred to the 0′ system. Let there be an incident plane wave of unit strength and characterized by a wave vector $\boldsymbol{k}$, an incident angle α with respect to the z axis, and a polarization angle γ between $\boldsymbol{E}$ and the projection of 00′ on the incident wavefront as shown in Fig. 1. Then, following Stratton's notations [16] for vector spherical wave functions, the total electric field expanded with respect to 0 [7]–[9], [12] can be written as,[1] for $r \geq a$,

$$\begin{aligned}\boldsymbol{E}_T = \sum_{n,m} [&p(m,n)\boldsymbol{N}_{mn}^{(1)} + q(m,n)\boldsymbol{M}_{mn}^{(1)} \\ &+ A_E(m,n)\boldsymbol{N}_{mn}^{(3)} + A_H(m,n)\boldsymbol{M}_{mn}^{(3)} \\ &+ B_E(m,n)\sum_{\nu}(A_{m\nu}^{mn}\boldsymbol{N}_{m\nu}^{(1)} + B_{m\nu}^{mn}\boldsymbol{M}_{m\nu}^{(1)}) \\ &+ B_H(m,n)\sum_{\nu}(A_{m\nu}^{mn}\boldsymbol{M}_{m\nu}^{(1)} + B_{m\nu}^{mn}\boldsymbol{N}_{m\nu}^{(1)})] \quad (1)\end{aligned}$$

where $p(m,n)$ and $q(m,n)$ are multipole coefficients of the incident plane wave

$$p(m,n) = i^{n+1}\frac{2n+1}{n(n+1)}\frac{(n-m)!}{(n+m)!} \cdot [\pi_{mn}(\alpha)\cos\gamma + i\tau_{mn}(\alpha)\sin\gamma] \quad (2)$$

$$q(m,n) = i^{n+1}\frac{2n+1}{n(n+1)}\frac{(n-m)!}{(n+m)!} \cdot [\tau_{mn}(\alpha)\cos\gamma + i\pi_{mn}(\alpha)\sin\gamma] \quad (3)$$

$$\pi_{mn}(\alpha) = \partial_\alpha P_n^m(\cos\alpha), \quad \tau_{mn}(\alpha) = \frac{m}{\sin\alpha}P_n^m(\cos\alpha) \quad (4)$$

[1] Time variation $\exp(-i\omega t)$ is assumed. $\partial_\alpha = \partial/\partial\alpha$.

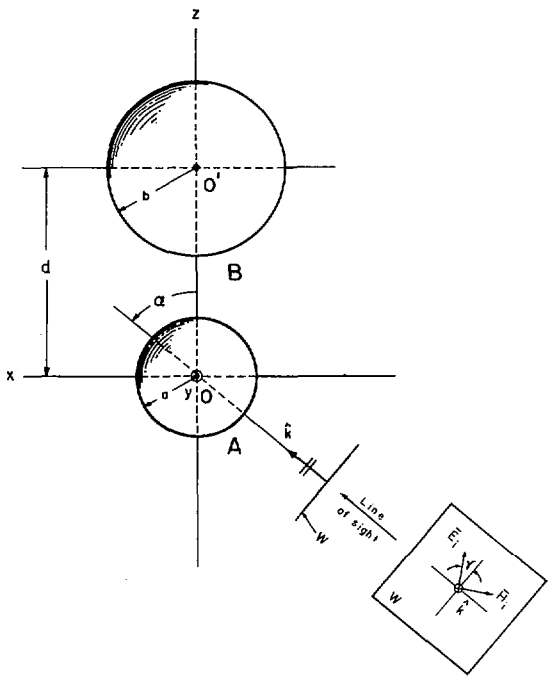

Fig. 1. Geometry of two-sphere problem.

$\boldsymbol{N}_{mn}^{(j)}, \boldsymbol{M}_{mn}^{(j)}$ are vector spherical wave functions

$$\boldsymbol{M}_{mn}^{(j)} = z_n^{(j)}(kr)\,(\exp im\phi) \cdot\left[\frac{im}{\sin\theta}P_n^m(\cos\theta)\hat{\boldsymbol{\theta}} - \partial_\theta P_n^m(\cos\theta)\hat{\boldsymbol{\phi}}\right] \quad (5)$$

$$\boldsymbol{N}_{mn}^{(j)} = \frac{1}{kr}z_n^{(j)}(kr)\,(\exp im\phi)n(n+1)P_n^m(\cos\theta)\boldsymbol{r} + \frac{1}{kr}\partial_r[rz_n^{(j)}(kr)]\,(\exp im\phi) \cdot\left[\partial_\theta P_n^m(\cos\theta)\hat{\boldsymbol{\theta}} + \frac{im}{\sin\theta}P_n^m(\cos\theta)\hat{\boldsymbol{\phi}}\right] \quad (6)$$

where $z_n^{(j)}$ is the appropriate kind of spherical Bessel functions j_n, n_n, $h_n^{(1)}$, and $h_n^{(2)}$, for $j = 1, 2, 3$, and 4, respectively; A_E, A_H, B_E, B_H are "multipole coefficients" of E and H waves scattered, respectively, by spheres A and B in the presence of each other; and $A_{m\nu}^{mn}, B_{m\nu}^{mn}$ are "translation coefficients" of the vector spherical wave functions from 0′ to 0. (See the Appendix for details).

There is a similar expression for $\boldsymbol{E}_T'$ with respect to the 0′ system, for which the multipole coefficient of the incident plane wave $p'(m,n)$ and $q'(m,n)$ differ from $p(m,n)$ and $q(m,n)$ by a factor $\exp ikd\cos\alpha$, and $A'_{m\nu}{}^{mn}$ and $B'_{m\nu}{}^{mn}$ differ from $A_{m\nu}{}^{mn}$ and $B_{m\nu}{}^{mn}$ by $(-1)^{n+\nu}$ and $(-1)^{n+\nu+1}$, respectively. The total magnetic field $\boldsymbol{H}_T$ is obtained by interchanging $\boldsymbol{N}_{mn}$ and $\boldsymbol{M}_{mn}$ in (1) and multiplying the result by $-ik/\omega\mu$.

By applying the appropriate boundary conditions and using the orthogonality properties of the Legendre functions, we arrive at four sets of coupled, linear, simultaneous equations in the unknown coefficients:

$$A_E(m,n) = v_n(k_1,ka)\{p(m,n) + \sum_\nu [A_{mn}^{m\nu}B_E(m,\nu) + B_{mn}^{m\nu}B_H(m,\nu)]\}$$

$$A_H(m,n) = u_n(k_1,ka)\{q(m,n) + \sum_\nu [A_{mn}^{m\nu}B_H(m,\nu) + B_{mn}^{m\nu}B_E(m,\nu)]\}$$

$$B_E(m,n) = v_n(k_2,kb)\{p'(m,n) + \sum_\nu (-1)^{n+\nu} \cdot [A_{mn}^{m\nu}A_E(m,\nu) - B_{mn}^{m\nu}A_H(m,\nu)]\}$$

$$B_H(m,n) = u_n(k_2,kb)\{q'(m,n) + \sum_\nu (-1)^{n+\nu} \cdot [A_{mn}^{m\nu}A_H(m,\nu) - B_{mn}^{m\nu}A_E(m,\nu)]\}. \quad (7)$$

The coefficients $v_n(k_1,ka)$, $u_n(k_1,ka)$, $v_n(k_2,kb)$, and $u_n(k_2,kb)$ are, respectively, the classical electric and magnetic multipole coefficients of the external field of spheres A and B in isolation. k, k_1, and k_2, are the wavenumbers in the surrounding medium, sphere A, and sphere B, respectively.

It should be emphasized that the system (7) is valid for determination of the multipole coefficients for the scattering by any pair of spheres, equal or unequal in size, of the same or different material as long as the appropriate single sphere coefficients u_n and v_n for each sphere are known.[2]

It is clear from (7) that there is no coupling among the azimuthal modes (i.e., modes with different index m); hence, this system of equations may be solved independently for each m where $-n \leq m \leq n$, and represents in general, $2n + 1$ sets of equations. As shown later, there are several important special cases in which the form of (7) can be simplified considerably.

Scattered Far Field and Various Approximate Solutions

Of practical interest is the scattered field in the far zone of the ensemble of two spheres which may, nevertheless, be in the near field of each other. This is obtained from the asymptotic forms of the vector spherical wave functions for $r, r' \gg d$. By observing the symmetry inherent in the coefficients and the wave functions, all previous field expressions can be transformed into series involving only nonnegative values of the index m if the incident field is decomposed into its horizontal and vertical components which yields a great computational advantage. Thus, for the two principal polarizations

$$\gamma = \begin{bmatrix} 0 \\ \pi/2 \end{bmatrix}$$

the far field scattered by both spheres referred to origin 0 is given by

$$\boldsymbol{E}_s^{A+B} \approx \frac{\exp ikr}{kr} \sum_{n=1}^{\infty} \sum_{m=0}^{n} i^{-n}\epsilon_m \cdot \left\{ [e(m,n)\pi_{mn}(\theta) + h(m,n)\tau_{mn}(\theta)] \begin{bmatrix} \cos m\phi \\ i \sin m\phi \end{bmatrix} \hat{\boldsymbol{\theta}} + i[e(m,n)\tau_{mn}(\theta) + h(m,n)\pi_{mn}(\theta)] \cdot \begin{bmatrix} i \sin m\phi \\ \cos m\phi \end{bmatrix} \hat{\boldsymbol{\phi}} \right\} \quad (8)$$

where ϵ_m is Neumann's number and

$$e(m,n) = A_E(m,n) + B_E(m,n) \exp(-ikd \cos\alpha)$$

$$h(m,n) = A_H(m,n) + B_H(m,n) \exp(-ikd \cos\alpha). \quad (9)$$

Note that $e(m,n)$ and $h(m,n)$ are also dependent on γ by virtue of (2), (3), and (7).

There are several instances in which the analysis may be simplified further by imposing certain additional restrictions.

1) The first involves the case of axial symmetry, i.e., when the propagation direction of the incident field coincides with the axis of the two spheres (endfire incidence $\alpha = 0$). As a consequence, the coefficients (2) and (3) of the incident field become

$$p(m,n) = q(m,n) = i^{n+1}\frac{2n+1}{2n(n+1)}\delta_{m,1}\begin{bmatrix} 1 \\ i \end{bmatrix}, \quad \gamma = \begin{bmatrix} 0 \\ \pi/2 \end{bmatrix} \quad (10)$$

where $\delta_{m,1}$ is the Kronecker delta. This means that the system (7) need be solved only for $m = 1$, where the coefficients $A_{1\nu}^{1n}$ and $B_{1\nu}^{1n}$ assume a particularly simple form [12].

2) Another simplification involves identical spheres at broadside incidence ($a = b$, $\alpha = \pi/2$) where it may be shown that the coefficients of the spheres bear the simple relation

$$B_E(m,n) = \mp(-1)^{n+m}A_E(m,n)$$

$$B_H(m,n) = \pm(-1)^{n+m}A_H(m,n). \quad (11)$$

The upper and lower signs refer, respectively, to the incident polarizations $\gamma = 0, \pi/2$. With this simplification, (7) reduces to two coupled sets of equations [12].

3) The Rayleigh approximation gives rise to a particularly simple form, since this situation is characterized by

[2] The precise form for u_n and v_n is also known for spheres composed of several concentric layers of different materials [13] or concentric layers of nonuniform dielectric constant [24].

the assumption that ka and kb are so small that only the terms for $n = 1$ contribute, the others being taken as zero. This case has previously been considered by several authors using Trinks' formulation [1], [2], [4], [6]. The explicit low-order translation coefficients are simply inserted into (7), which is then solved algebraically [12].

4) Lastly, a very useful approximation is obtained for the case where each sphere is situated in each others' far field. This is satisfied when $d/x > 0(kx)$, where x is the larger of a and b. In this case, it can be shown that the addition theorem takes a very simple form [12]. From this, we find that the system may be uncoupled and solved analytically. This is accomplished by successive substitution and noting that in the process we are generating geometric series which can be summed (after a considerable amount of bookkeeping) in closed form. For illustration, consider the vertical polarization ($\gamma = \pi/2$), and scattering in the plane $\phi = \pi$. With the identifications

$$s_\phi{}^A = \frac{\Phi S_\phi{}^b(d,\pi - \alpha,0) + S_\phi{}^a(d,\alpha,\pi) S_\phi{}^b(d,\pi,\pi)}{1 - S_\phi{}^a(d,\pi,\pi) S_\phi{}^b(d,\pi,\pi)}$$

$$s_\phi{}^B = \frac{\Phi^* S_\phi{}^a(d,\alpha,\pi) + S_\phi{}^b(d,\pi - \alpha,0) S_\phi{}^a(d,\pi,\pi)}{1 - S_\phi{}^a(d,\pi,\pi) S_\phi{}^b(d,\pi,\pi)}$$

$$\Phi = \exp(ikd \cos\alpha) \tag{12}$$

and

$$S_\phi{}^z(r,\theta,\phi) = \frac{\exp ikr}{ikr} \cdot \sum_{n=1}^{\infty} [u_n(kx)\pi_{1n}(\theta) + v_n(kx)\tau_{1n}(\theta)] \cos\phi \tag{13}$$

we arrive at [12]

$$E_\phi{}^{A+B} = S_\phi{}^a(r,\theta + \alpha,\pi) + S_\phi{}^b(r,\theta + \alpha,\pi) \exp i\delta + s_\phi{}^B S_\phi{}^a(r,\pi - \theta,0) + s_\phi{}^A S_\phi{}^b(r,\theta,\pi) \exp i\delta \tag{14}$$

where $\delta = kd(\cos\alpha - \cos\theta)$. Inspection of (12)–(14) reminds us that we have a result composed only of single sphere scattering amplitudes. Furthermore, this result was obtained only by using the far field form of the addition theorem.

The scattering amplitudes $s_\phi{}^A$ and $s_\phi{}^B$ have an enlightening interpretation with the aid of Fig. 2. $s_\phi{}^A$, for example, is the strength of a field incident on B from A. Its amplitude is composed of the first-order field scattered by B toward A: $\Phi S_\phi{}^b(d,\pi - \alpha,0)$ and a field scattered by A toward B and then backscattered by B: $S_\phi{}^a(d,\alpha,\pi) S_\phi{}^b(d,\pi,\pi)$. The term $[1 - S_\phi{}^a(d,\pi,\pi) S_\phi{}^b(d,\pi,\pi)]^{-1}$ multiplying the aforementioned amplitudes is the effect of all higher order "bounces" of these two amplitudes, which we note is the sum of a geometric series in powers of the term $S_\phi{}^a(d,\pi,\pi) S_\phi{}^b(d,\pi,\pi)$; its convergence is assured by the initial assumption of each sphere being in the others' far field. For two identical spheres at broadside incidence, (14) becomes ($\gamma = \pi/2$)

$$E_\phi{}^{A+B} = 2\left[S_\phi{}^a(r,\pi,\pi) - \frac{S_\phi{}^a(r,\pi/2,\pi) S_\phi{}^a(d,\pi/2,\pi)}{1 + S_\phi{}^a(d,\pi,\pi)}\right]. \tag{15}$$

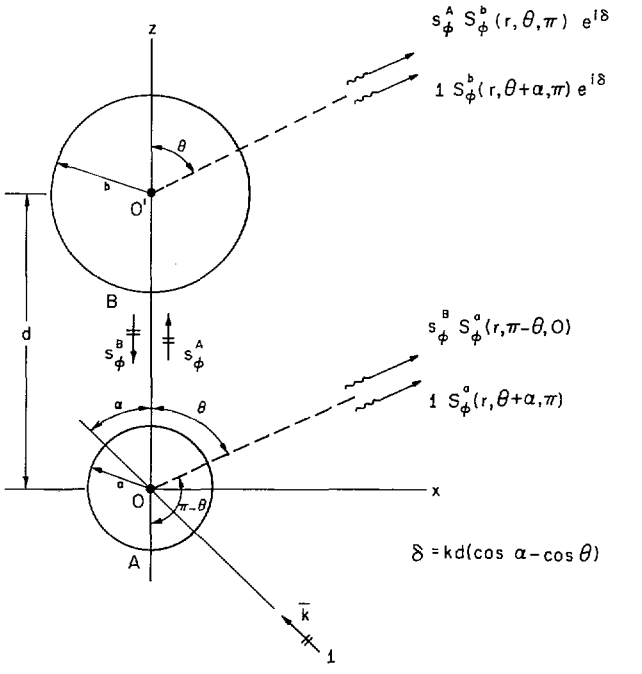

Fig. 2. Interpretation of multiply scattered fields in (12) and (14).

It is interesting to note that this approximation yields surprisingly good results even for two spheres in contact. This is shown in Fig. 3, where the normalized radar cross sections (RCSs) for various sizes of conducting spheres are plotted, the solid curves being obtained from the exact solution.

Ray-Optical Solution

Levy and Keller [17] elegantly extended Franz's creeping wave theory [18] for the sphere to scattering by an arbitrary smooth convex body. Ray paths associated with the creeping waves obey Fermat's principle and hence, lie along geodesics of the surface. While their approach to the electromagnetic (EM) problem makes use of two scalar acoustic problems, here we are concerned specifically with the behavior of the vector problem of the sphere. Senior and Goodrich [19] expressed the single sphere scattered field in a form which makes identification of the appropriate diffraction and attenuation coefficients an easy matter.

The rays which contribute to the scattered field of the two sphere ensemble fall into three categories: 1) reflected rays arising from direct and multiple reflections, 2) creeping wave rays bound to a single body, and 3) "hybrid rays" [12], [20]. The rays falling into the last category

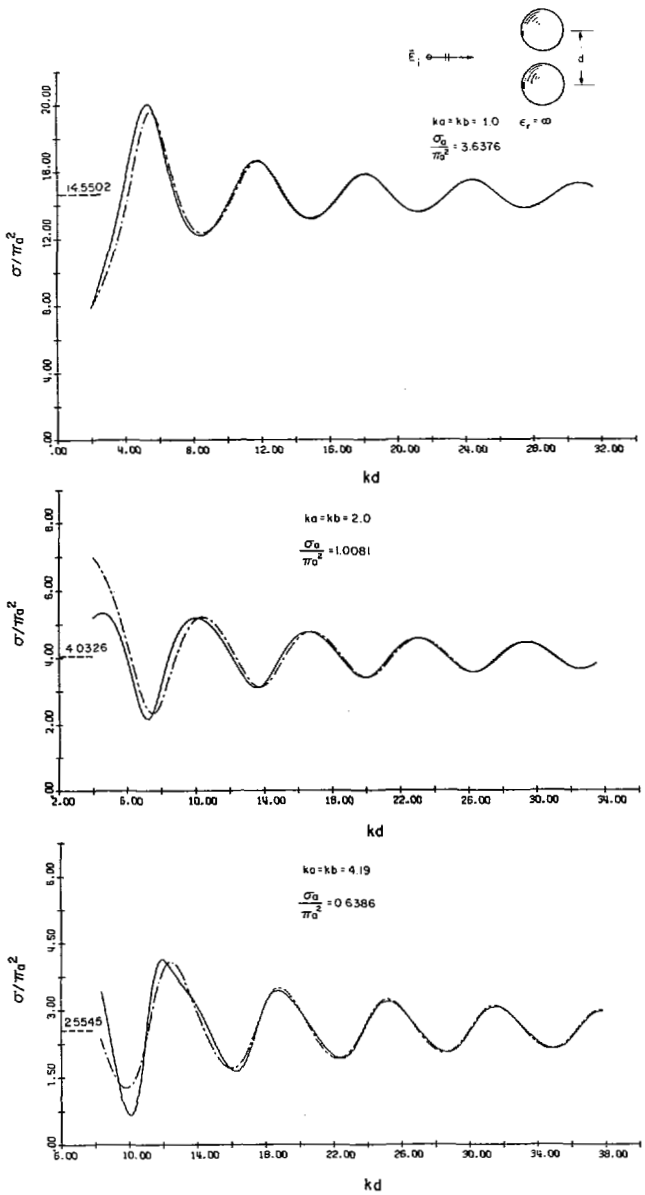

Fig. 3. RCS of two equal metallic spheres at broadside incidence for $ka = 1.0$, 2.0, and 4.19 using exact solution (———) and asymptotic form (15) for large separation (—·—·).

are those which involve any combination of rays of the first two types. For purposes of further classification, rays of the first type which undergo j reflections are denoted by R_j; those rays of the second type which creep over a length equal to or less than halfway around the body are denoted by C_-; C_+ describes the case of a larger length. Finally, the third case may be represented by any combination of the preceding symbols with its obvious implication. For example, a ray which creeps part way around one sphere, most of the way around the other, and reflects five times between the two before reaching the observer may be identified by the symbol $C_-C_+R_5$. A particular geometry of two spheres could support any number of configurations of rays; however, generally only a few will be significant.

Field calculations employing the geometric optics approximation are carried out using Snell's Law and the conservation of energy. If $E(A)$ is the value of the incident field at a point A, then the reflected field at some point P, a distance S from A, is given by

$$E(P) = -E(A)\left[\frac{\rho_1\rho_2}{(\rho_1 + S)(\rho_2 + S)}\right]^{1/2} \exp ikS \quad (16)$$

where ρ_1 and ρ_2 are the principal radii of curvature of the wavefront reflected from A. The bracketed term is designated the divergence factor Δ. If more than one reflection is involved, the preceding procedure is repeated; the field at some point P after N reflections will then assume the form

$$E(P) = (-1)^N E(A) \prod_{r=1}^{N} \Delta_r \exp ikS_{rN}.$$

For simplicity we will consider the scattered field at the point in the plane of incidence as shown in Fig. 4, where only the member R_2 of the set $\{R_j\}$ is drawn. R_2 consists of the subrays $S_{02} - S_{12} - S_{22}$. In general, a member of $\{R_j\}$ comprises $S_{0j} - S_{1j} - \cdots - S_{jj}$ where S_{ij} is used to denote the length of the ray between reflection points i and $i + 1$. The angle between ray S_{ij} and the normal at the ith reflection point is denoted by η_{ij}. Then, for the assumed incident plane wave, the far field due to one reflection R_1 from sphere A is

$$R_1 = -\frac{a}{2r} \exp ik(R + r - 2a\cos\eta_{11}) \quad (17)$$

where

$$r = S_{11} + a\sin\eta_{11}, \qquad \eta_{11} = \frac{\pi - \theta - \alpha}{2}.$$

θ is the polar angle of observation point P, and R is the distance from the source to origin 0. We have a similar expression for sphere B.

For two reflections, one must first determine the three unknowns η_{12}, η_{22}, and S_{12} [12]. Once these parameters are determined, the divergence factors Δ_i may be calculated. The result analogous to (17) for two reflections is given by [12]

$$R_2 = \frac{ab}{2r}\left[\frac{\cos\eta_{12}\cos\eta_{22}}{(l_1\cos\eta_{22} + l_2\cos\eta_{12})(\bar{l}_1 + \bar{l}_2)}\right]^{1/2} \cdot \exp ik[R - a\cos\eta_{12} + S_{12} + r - b\cos\eta_{22} - d\cos\theta] \quad (18)$$

where $r = S_{22} + b\cos\eta_{12} + d\cos\theta$ and

$$l_1 = a + S_{12}\cos\eta_{12}, \quad \bar{l}_1 = S_{12} + a\cos\eta_{12}$$
$$l_2 = b + S_{12}\cos\eta_{22}, \quad \bar{l}_2 = S_{12} + b\cos\eta_{22}.$$

There is, of course, a companion ray which reflects off of sphere B first and then A before reaching the observer. This may be calculated from the preceding by making a

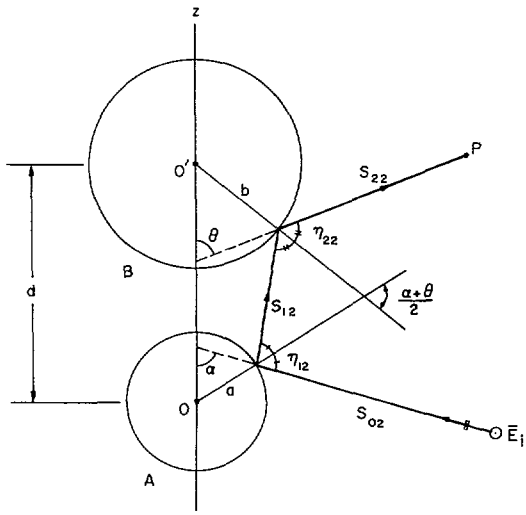

Fig. 4. Geometry of two-sphere problem showing ray that undergoes two reflections.

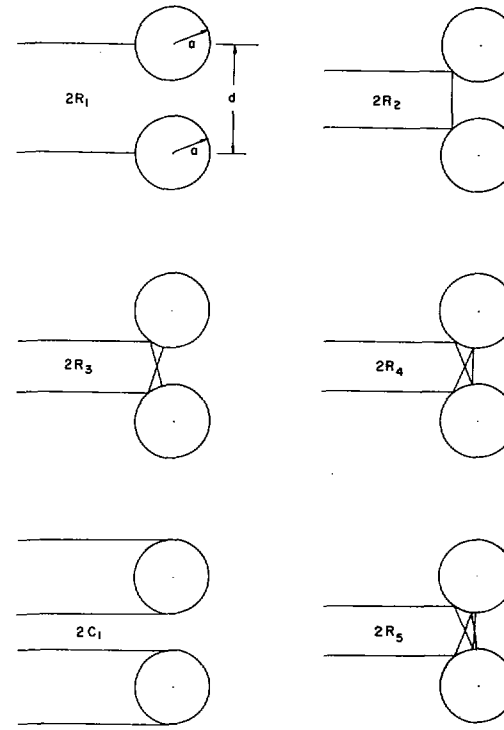

Fig. 5. Some rays which contribute to backscattered field of two spheres illuminated from broadside direction.

few obvious changes. We could carry out the same type of analysis for a field that has undergone j reflections before reaching the observer, but the analysis becomes rapidly more complicated since there will be, in general, $2j - 1$ unknowns involved in the form of simultaneous transcendental equations.

It is quite difficult to describe a general hybrid ray in the same sense as we did for the multiple reflected rays since it can assume any number of forms comprising creeping wave rays and reflected rays. However, generally, only a few contribute significantly to the scattered field in a particular direction. It is perhaps more meaningful in describing the role of these different types of multiple scattered rays if we consider one case in which the dominant multiple scattering mechanism is multiple reflection and another in which it is hybrid rays. In the first case we consider the backscattered field from a pair of identical metallic spheres illuminated from the broadside direction, and, in the latter case, from the endfire direction.

Broadside Incidence ($\alpha = \pi/2$)

Consider first the case of a pair of identical perfectly conducting spheres of radius a illuminated by a plane wave perpendicular to their common axis, $\alpha = \pi/2$. For this discussion, we will be interested only in the backscattered field. Some of the rays appropriate for this geometry are shown in Fig. 5. The most significant hybrid rays for this configuration, even though there are four, $(2C_-R_1 + 2R_1C_-)$, contribute negligibly except for small spheres.

Returning to the reflected rays, the contribution due to R_1 is already given in (17) with $\eta_{11} = 0$. For R_2, since $\eta_{12} = \eta_{22} = \pi/4$ with $S_{12} = d - a\sqrt{2}$, from (18),

$$R_2 = \pm \frac{R_1}{2\mu(1 - 1/\sqrt{2}\mu)^{1/2}} \exp ika(\mu + 2 - 2\sqrt{2}) \quad (19)$$

where $\mu = d/a$ and the upper and lower signs refer, respectively, to horizontal and vertical polarization ($\gamma = 0$, $\pi/2$). This result was also obtained by Bonkowski, *et al.* [21] using a lengthy tensor formulation. The expressions for the fields which have undergone three, four, five, and more reflections have also been derived [12] but need not be written down since the expressions become lengthy and the recipe for obtaining them has already been given.

As one would expect, the contribution of the reflected ray decreases with its order. In Fig. 6, the modulus of the multiply reflected rays R_2 through R_7 (normalized to R_1 as in (19)), is shown for several values of the ratio d/a. The general behavior is perhaps more vividly illustrated by the spot pictures adjacent to each curve. These photos were obtained by photographically recording the light intensity (square of modulus) reflected by two polished silvered spheres. The two bright spots, common to all the diagrams, denote the specular returns R_1 from the front surface of each sphere. The remaining spots $R_2, R_3, \cdots$, (when they can be seen) are identified by counting inward from the two R_1 spots. Each picture was obtained by illuminating the pair of spheres shown in the top photo by a point source of ordinary light situated close to the axis of the camera and recording the reflected intensity on film when the studio lights were extinguished. Due to the limited exposure, only those spots of intensity greater than -30 dB with respect to R_1 can be seen. From this figure, we observe that when the spheres are separated by as little as one diameter ($d/a = 4.0$), the magnitudes of succeeding higher order reflected rays differ nearly by an

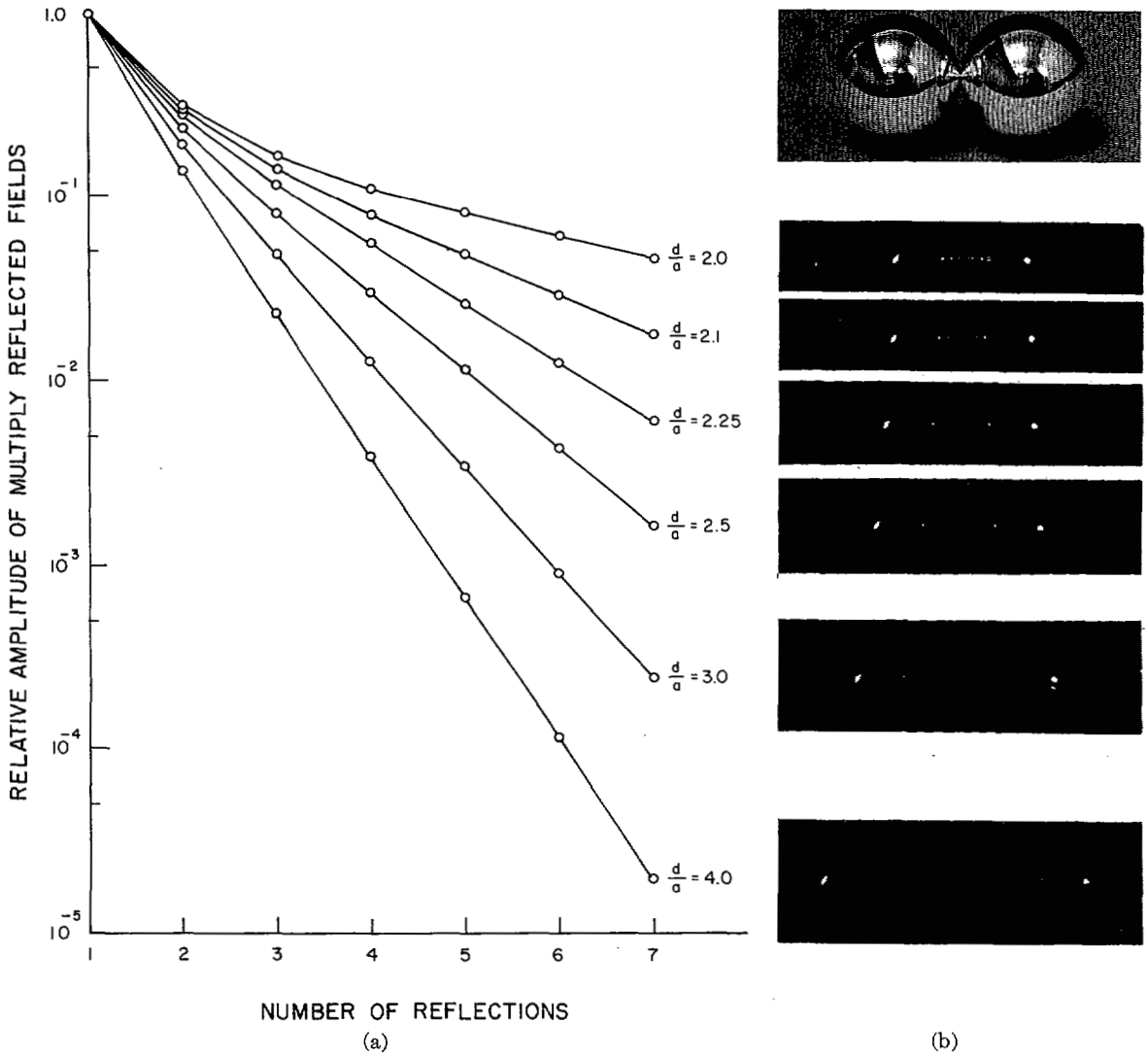

Fig. 6. Comparison of relative amplitudes of multiply reflected backscattered rays for various spacings at broadside incidence. (a) Obtained by computation. (b) Obtained by photographic method (see text).

order of magnitude; this is hardly the case when the spheres are in contact. It is worth remembering that the modulus of the multiple-reflected rays is a function of the ratio d/a, not the spacing d.

Using only the rays R_1, C_- and R_2 through R_6, we compute the normalized RCSs of pairs of identical metallic spheres for the two principal polarizations for $ka = 2.00$, 4.19, 6.246, and 10.00. This size range was chosen so that the results could be compared with those of the exact solution for the purpose of determining where solutions obtained by the two approaches "overlap," and also for comparison with some experimental results given in [25]. These results are presented in Fig. 7.

In the interest of comparing the two solutions as accurately as possible, Fig. 7 (and ones to follow) were drawn by a computer-controlled digital plotter. A large number of data points for each curve was fed to the plotting program and intermediate points were calculated by a piecewise cubic interpolation scheme. Curves comparing the two solutions were plotted at the same time on the same grid—the dashed curves always representing the ray optical solution and the solid curves, the exact solution unless otherwise stated.

With the exception of the case of horizontal polarization at $ka = 2.0$, the agreement is surprisingly good. From these figures, we also see that as d/a becomes large (and hence the coupling small), the normalized cross section settles down to $4\sigma_a/\pi a^2$ as expected, σ_a being the RCS of a single sphere.

A further example is given in Fig. 8, involving the RCS of a pair of spheres in contact as they both grow in size for vertical polarization. Again, the same set of rays is considered as was used for computation in the previous example. The creeping wave influence for this example is apparent for $ka \leq 10$ and can be identified with the local maxima in this range since we know the creeping wave C_- to add in phase with R_1 (for the single sphere) at $ka \approx 2n\pi/(2 + \pi)$, where n is a positive integer, and with a period in ka of roughly $2\pi/(2 + \pi)$. Beyond this point, the RCS is almost completely dominated by the geometric

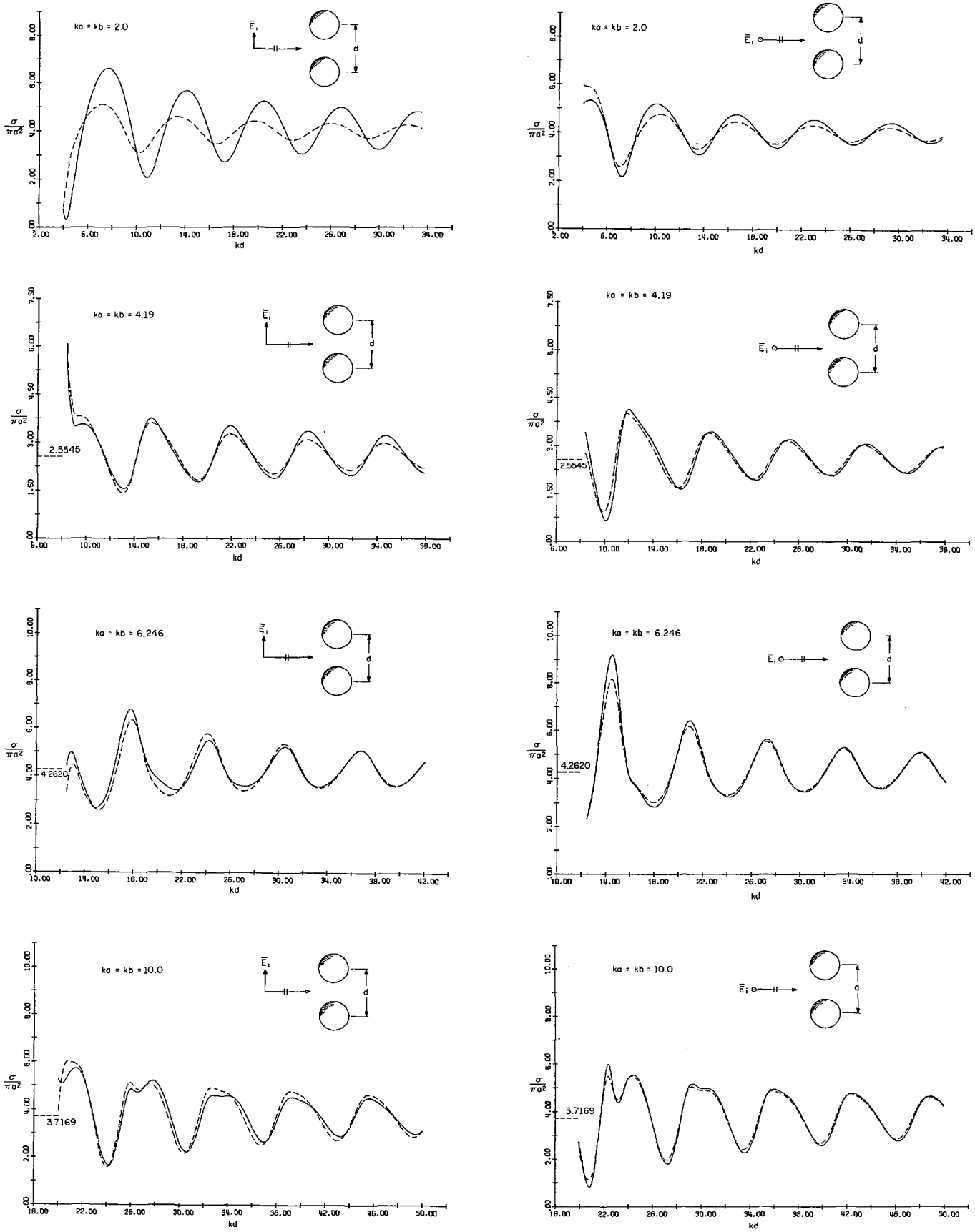

Fig. 7. RCS of two equal perfectly conducting spheres at broadside incidence as spacing is varied for $ka = 2.0$, 4.19, 6.246, and 10.0, comparing ray-optical solution (– – –) with exact solution (——).

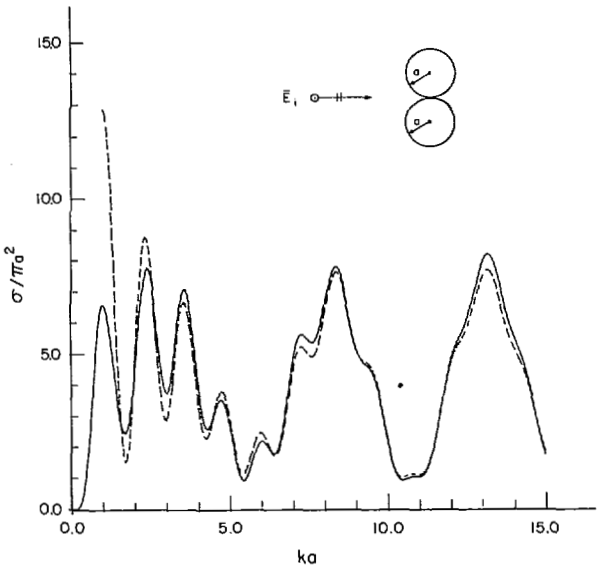

Fig. 8. RCS of two equal perfectly conducting spheres in contact at broadside incidence as sphere size increases, comparing ray optical solution (– – –) with exact solution (——).

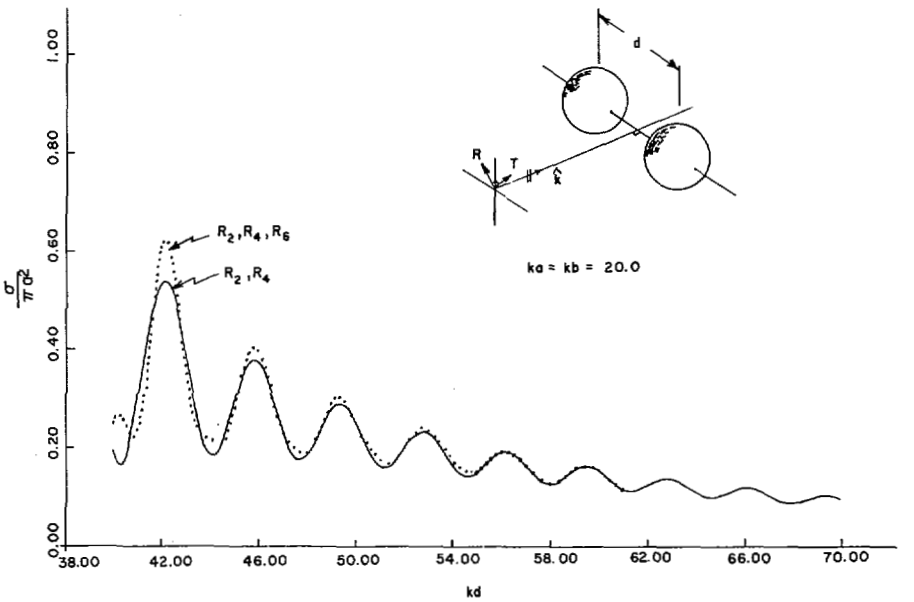

Fig. 9. Cross-polarized RCS from pair of equal perfectly conducting spheres $ka = 20.0$ as spacing is varied using rays R_2, R_4, and R_6. T and R indicate polarizations of incident and received E vectors, respectively.

optics components alone. The normalized RCS of the pair will not, however, settle down to some constant value for large ka as it does for the single sphere. This is because the ratio d/a is constant, and as a result, the normalized return is made up of components which are constant in magnitude; only the relative phases change with ka. Normally, we associate ray methods with problems in which characteristic dimensions are much larger than a wavelength. Here we find excellent agreement with the exact solution for a pair of spheres in contact even when the radii are as small as $\lambda/4$.

There is another configuration which, because of its practical application and simplicity, warrants mention. In this case, an identical pair of metallic spheres is illuminated from the broadside direction with a plane wave whose polarization vector makes an angle of 45° with the common axis of the two spheres ($\gamma = \pi/4$). Due to symmetry, only the even components, $R_2, R_4, \cdots, R_{2n}$, contribute to the cross-polarized radar return. A sample computation for a large pair of spheres ($ka = 20.0$) is shown in Fig. 9 where the effect of some of the higher order rays is readily seen. The simplicity of the analysis and configuration makes this an interesting method for cross-polarized RCS calibration. This is discussed more generally in [25] with further results.

Endfire Incidence ($\alpha = 0$)

In the case of endfire incidence, as shown in Fig. 10, the sphere B may lie wholly in the geometric shadow of A if $b \leq a$; hence, the only purely geometric return is the

specular reflection from sphere A. Some rays to consider for this geometry when $b = a$ are R_1, C_-, $C_-R_1{}^NC_-$, $C_-R_1C_-$, $C_-R_3{}^NC_-$, $C_-R_3C_-$, $C_-C_+C_-$, etc., where $R_j{}^N$ means that of j multiple reflections, one is a normal reflection. Strictly speaking, geometric optics dictates that the shadowed sphere will never see directly the incident field which we know it should eventually at very large spacing. As a result, the backscattered field of two identical spheres should eventually approach the single sphere value times the array factor $1 + \exp(2ikd)$.

The backscattered field due to the first two dominant hybrid rays for arbitrary a and b is

$$C_-R_1{}^NC_- = R_1 \frac{D_0^4}{a}\left[\frac{\tau\pi ka}{\mu^2 - 1 - \tau(\mu^2-1)^{1/2}}\right]^{1/2} \cdot\exp\left\{i2ka[1 - \tau + (\mu^2-1)^{1/2} + \csc^{-1}\mu] - \frac{i\pi}{4} - 2\alpha_0 a \csc^{-1}\mu\right\} \tag{20}$$

$$C_-R_1C_- = R_1(-i)\frac{D_0^4}{a}\left[\frac{\pi ka}{((\mu-\tau)^2-1)^{1/2}}\right]^{1/2} \cdot\exp\left\{i2ka[1 + ((\mu-\tau)^2-1)^{1/2} + \csc^{-1}(\mu-\tau)] - \frac{i\pi}{4} - 2\alpha_0 a \csc^{-1}(\mu-\tau)\right\} \tag{21}$$

where $\tau = b/a$ and $\mu = d/a$. (D_0^4/a) is the product of four surface diffraction coefficients and α_0 is the attenuation coefficient associated with the normal component of the field that creeps around the sphere [12].

Using the rays R_1, C_-, $C_-R_1{}^NC_-$, and $C_-R_1C_-$, shown schematically in Fig. 10, we compute the normalized RCS of two identical metallic spheres for $ka = 7.41$, 11.048, and 20.0. These results are shown in Fig. 11 together with the exact solution for comparison. In the absence of coupling, the normalized RCS will oscillate between 0 and $4\sigma_a/\pi a^2$ as kd is varied; this latter value is indicated by the dashed line on the ordinate for each case. The agreement gets better (for small to moderate d/a) with increasing ka as we would expect, and is best for $ka = 20.0$. The results even for $ka = 7.41$, however, are not very satisfactory. The discrepancy can be attributed, at least in part, to the inaccuracy in the canonical creeping wave problem near a shadow boundary.

Let us consider computing the normalized RCS of two identical metallic spheres in contact at endfire incidence as they both grow in size using only the rays R_1 and $C_-R_1{}^NC_-$. It may be recalled that the creeping wave influence on the backscattering from a single sphere is nearly absent at values of ka greater than about 10–15 due to its large attenuation. Placing an identical sphere directly

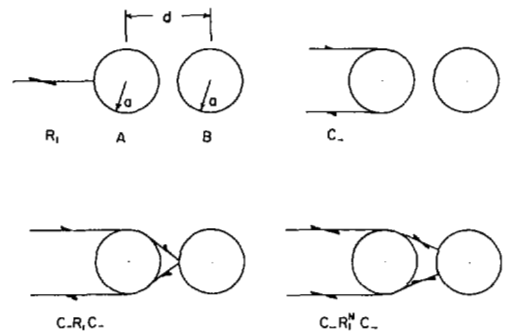

Fig. 10. Most significant rays for backscattering at endfire incidence and close spacing.

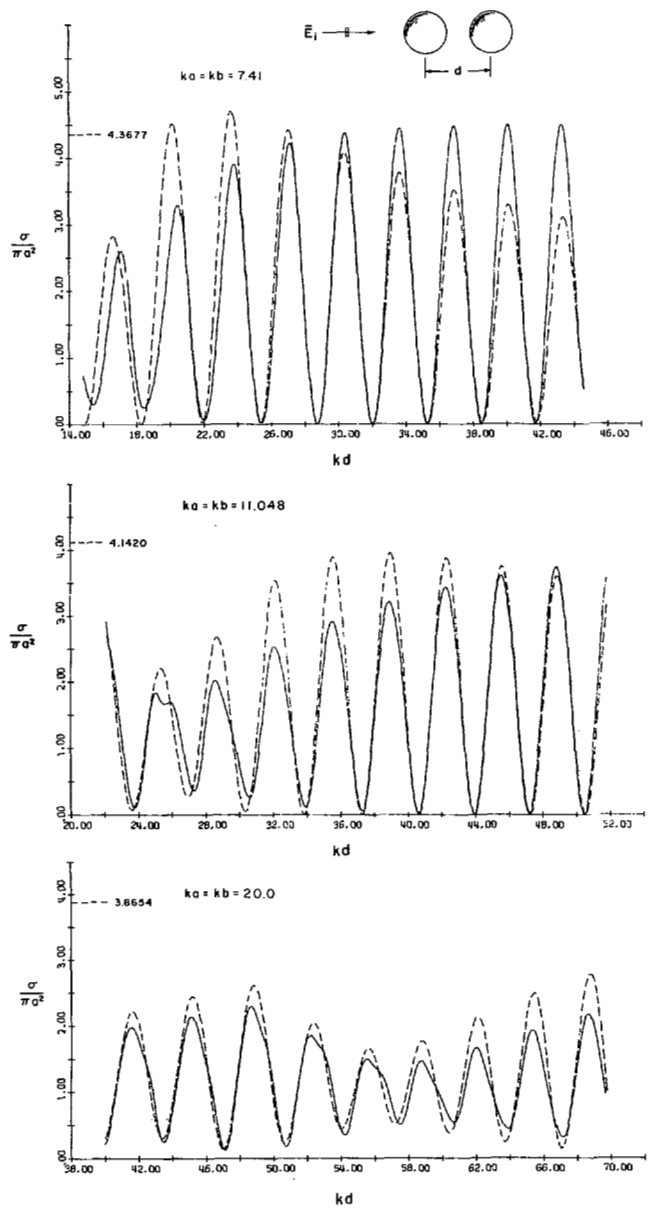

Fig. 11. RCS of two equal perfectly conducting spheres at endfire incidence as spacing is varied for $ka = 7.41$, 11.048, 20.0, comparing ray-optical solution (– – –) and exact solution (——).

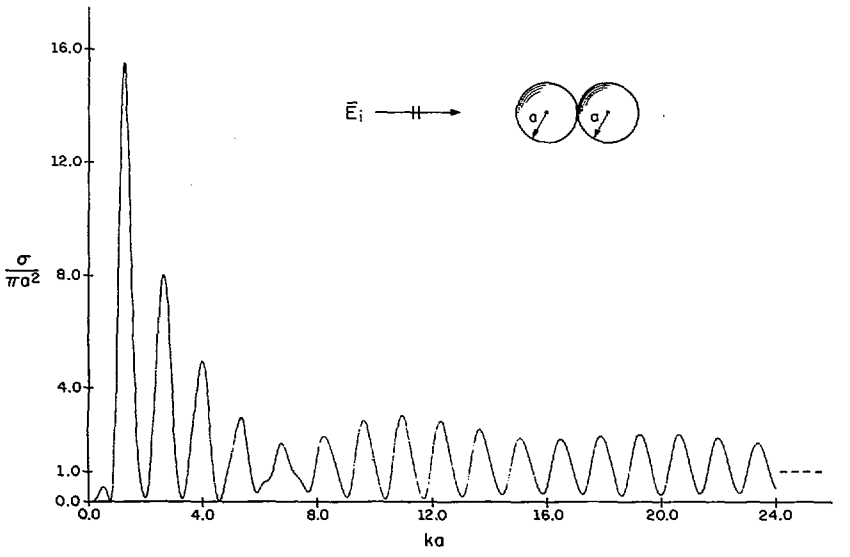

(a)

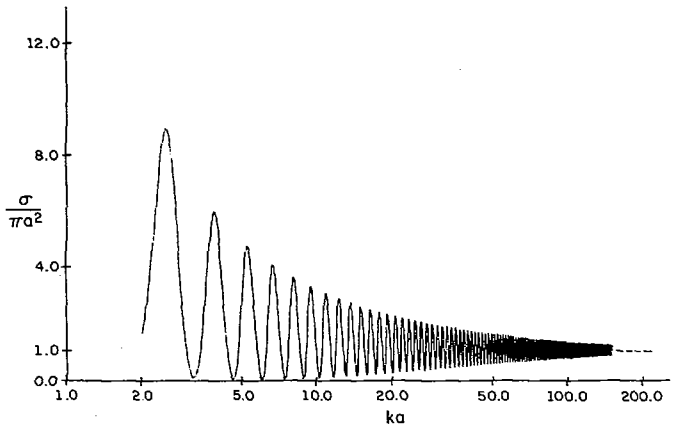

(b)

Fig. 12. RCS of two equal perfectly conducting spheres at endfire incidence in contact as sphere size increases. (a) Exact solution. (b) Ray-optical solution.

behind a previously isolated sphere drastically alters the situation, since the hybrid wave $C_-R_1^NC_-$ overwhelms any single sphere creeping wave C_-, and its associated creeping path length is only a total of one sixth of the circumference of the first sphere, implying that the oscillations about R_1 will persist for a much larger value of ka than for the single sphere. In Fig. 12(a) the normalized RCS of a pair of identical spheres in contact is shown, computed by the multipole expansion approach as ka covers the range 0 to 24. It is clearly seen that there is considerable oscillation about R_1 even for ka as large as 24. It becomes somewhat costly to carry out computations much beyond this value using the modal approach. Therefore, we must resort to ray optics. Fig. 12(b) shows the ray-optical solution to the same problem plotted logarithmically in ka to $ka = 150$. If we compare these two curves, we find excellent agreement in the location of the peaks and nulls after $ka \approx 10$ and also in the amplitude after $ka \approx 16$. The period of oscillation can be very simply determined. Knowing that these oscillations are caused only by the interference of R_1 and $C_-R_1^NC_-$, the period P, in ka, of the oscillation can be shown from (20) to be simply $\pi/(\pi/6 + \sqrt{3}) \approx 1.39$, with peaks at $ka = nP$ and nulls at $ka = (2n - 1)P/2$ where n is a positive integer.[3]

It is interesting to note from the geometric optics point of view that eventually the front sphere can "hide" the back sphere at sufficiently high frequency. In fact, the front sphere may even hide a sphere that is larger than itself. Since the attenuation of the hybrid rays $C_-R_1^NC_-$ is proportional to $\exp(-2\alpha_0 a \csc^{-1}\mu)$, ka must be larger in order to hide a bigger sphere ($b > a$) than to hide a smaller one ($b < a$).

Conclusion and Discussion

The problem of electromagnetic scattering by two spheres has been solved through two approaches: multipole expansion and ray optics. Numerical results show that the former solution is useful even for spheres as large as 10λ in radius whereas the latter is useful for spheres as

[3] Note this is longer than the period of oscillations in the RCS curve for a single sphere which is $2\pi/(2 + \pi) \approx 1.23$.

small as $\lambda/4$ in radius in some cases. The former solution is very general and applicable to spheres of any material, but the latter is so far confined to conducting spheres. The ray-optical solution agrees very closely with that of the multipole expansion for relatively small spheres in the case of broadside incidence, but for much larger spheres in the endfire incidence case. Even for broadside incidence, the accuracy of the ray-optical solution of small spheres may be good for one polarization while poor for another polarization. This simply illustrates that care must be exercised in using the ray-optical approach. Despite this, it often gives us much physical insight into the problem.

Extension of the solution to scattering of acoustic waves by two spheres is straightforward. Interested readers are referred to [12]. It is perhaps of interest to point out that in the case of endfire incidence, the solution converges considerably slower than that for the case of EM waves due to stronger creeping wave coupling. It is also possible to extend these solutions to three or more collinear spheres. This, as well as many other theoretical results, are discussed in [25] where an unusually good agreement with the experiments will be seen.

Appendix

Translational Addition Theorem for Vector Spherical Wave Functions

In order to express vector spherical wave functions about a displaced origin 0′ in terms of wave functions about another origin 0, we employ the addition theorem:

$$\boldsymbol{M}_{mn}^{(j)\prime} = \sum_{\nu=(1,m)}^{\infty} [A_{m\nu}^{mn}\boldsymbol{M}_{m\nu}^{(1)} + B_{m\nu}^{mn}\boldsymbol{N}_{m\nu}^{(1)}]$$

$$\boldsymbol{N}_{mn}^{(j)\prime} = \sum_{\nu=(1,m)}^{\infty} [A_{m\nu}^{mn}\boldsymbol{N}_{m\nu}^{(1)} + B_{m\nu}^{mn}\boldsymbol{M}_{m\nu}^{(1)}]. \quad (22)$$

This applies to a translation along the z axis a distance d as in Fig. 1. When translating from 0′ to 0, $A_{m\nu}^{mn}$ and $B_{m\nu}^{mn}$ are preceded by the factors $(-1)^{m+\nu}$ and $(-1)^{m+\nu+1}$, respectively. For translation in any other direction, the theorem is somewhat more complicated and may be found elsewhere [12]–[14]. The wave functions are defined in (5) and (6), and the translation coefficients are given by [12]

$$A_{m\nu}^{mn} = (-1)^m i^{\nu-n}\frac{2\nu+1}{2\nu(\nu+1)} \cdot\sum_p i^{-p}[n(n+1)+\nu(\nu+1)-p(p+1)] \cdot a(m,n,-m,\nu,p)\begin{Bmatrix} z_p^{(j)}(kd) \\ j_p(kd)\end{Bmatrix}$$

$$B_{m\nu}^{mn} = (-1)^{m} i^{\nu-n}\frac{2\nu+1}{2\nu(\nu+1)}\sum_p i^{-p}(-2imkd) \cdot a(m,n,-m,\nu,p)\begin{Bmatrix} z_p^{(j)}(kd) \\ j_p(kd)\end{Bmatrix}, \quad \text{for} \begin{Bmatrix} r \le d \\ r \ge d\end{Bmatrix}. \quad (23)$$

The summation over p is finite covering the range $|n-\nu|, |n-\nu|+2, \cdots, (n+\nu)$, and includes $1+\max\{\nu,n\}$ terms. The preceding coefficients are further complicated by the presence of the coefficients $a(m,n,-m,\nu,p)$ which are defined by the linearization expansion

$$P_n^m(x)P_\nu^{-m}(x) = \sum_p a(m,n,-m,\nu,p)P_p(x). \quad (24)$$

These latter coefficients may be identified with a product of two 3-j symbols [13], [14], [22] which are associated with the coupling of two angular momentum eigenvectors:

$$a(m,n,-m,\nu,p) = (2p+1)\left[\frac{(n+m)!(\nu-m)!}{(n-m)!(\nu+m)!}\right]^{1/2} \cdot\begin{pmatrix} n & \nu & p \\ 0 & 0 & 0\end{pmatrix}\begin{pmatrix} n & \nu & p \\ m & -m & 0\end{pmatrix}. \quad (25)$$

The factor

$$\begin{pmatrix} j_1 & j_2 & j_3 \\ m_1 & m_2 & m_3\end{pmatrix}$$

is the Wignèr 3-j symbol of which there are several definitions, all involving summations of multitudes of factorials. As a result, straightforward calculation using (25) is very inefficient. In search of a better representation, inspection of the form of the coefficients $A_{m\nu}^{mn}$ and $B_{m\nu}^{mn}$ in (23) reveals that a recursion relation for the $a(\cdot)$ in which only the index p cycles would be highly desirable especially for machine computation. Just such a relation exists and is given by [12]

$$\alpha_{p-3}a_{p-4} - (\alpha_{p-2}+\alpha_{p-1}-4m^2)a_{p-2} + \alpha_p a_p = 0 \quad (26)$$

where

$$a_p \equiv a(m,n,-m,\nu,p), \quad p = n+\nu, n+\nu-2, \cdots, |n-\nu|$$

and

$$\alpha_p = \frac{[(n+\nu+1)^2-p^2][p^2-(n-\nu)^2]}{4p^2-1}. \quad (27)$$

We need not be concerned with the question of stability of this recursion relation since all quantities are rational numbers.

The recursion relation (26) is most conveniently employed in the backward direction since we can find simple starting values for the coefficients at $p = n+\nu$ and $p = n+\nu-2$. By matching coefficients in highest powers of the argument in (24), we find

$$a_{n+\nu} = \frac{(2n-1)!!(2\nu-1)!!}{(2n+2\nu-1)!!}\frac{(n+\nu)!}{(n-m)!(\nu+m)!}$$

$$a_{n+\nu-2} = \frac{(2n+2\nu-3)}{(2n-1)(2\nu-1)(n+\nu)} \cdot[n\nu - m^2(2n+2\nu-1)]a_{n+\nu} \quad (28)$$

where $(2q-1)!! = (2q-1)(2q-3)\cdots 3\cdot 1; (-1)!! \equiv 1$. Note that in (26) every new coefficient makes use of all previously calculated quantities and only requires two additional evaluations of the quantity α_p. The starting values (28) are, of course, not calculated directly from (28), since the recurrent form of the factorials may be utilized by generating these in the proper sequence (with regard to n, ν, and m) starting from $n = \nu = 1$, $m = 0$, where the coefficients (28) are 2/3 and 1/3, respectively. We see that nowhere have we had to calculate a single 3-j coefficient.

Special Forms

When $m = 0$, (26) becomes a two-term recursion formula which leads to a closed expression for $a(0,n,0,\nu,p)$ [12]. The properties of the associated Legendre functions allow us to obtain a closed expression for $m = 1$ also, but no higher:

$$a(1,n,-1,\nu,p) = -\frac{2p+1}{2\nu(\nu+1)}\,\frac{n(n+1)+\nu(\nu+1)-p(p+1)}{n+\nu+p+1} \cdot \frac{\binom{-n+\nu+p}{\frac{-n+\nu+p}{2}}\binom{n-\nu+p}{\frac{n-\nu+p}{2}}\binom{n+\nu-p}{\frac{n+\nu-p}{2}}}{\binom{n+\nu+p}{\frac{n+\nu+p}{2}}}.$$

This expression is particularly useful as it corresponds to the case of endfire incidence.

References

[1] W. Trinks, "Zur vielfachstreuung an kleinen kugeln," *Ann. Phys.* (Leipzig), vol. 22, 1935, pp. 561–590.

[2] J. Mevel, "Contribution de le diffraction des ondes electromagnetiques par les spheres," *Ann. Phys.* (Paris), 1960, pp. 265–320.

[3] N. R. Zitron and S. N. Karp, "Higher-order approximations in multiple scattering: I—two-dimensional scalar case, and II—three dimensional scalar cases," *J. Math. Phys.*, vol. 2, 1961, pp. 394–406.

[4] O. A. Germogenova, "The scattering of a plane electromagnetic wave by two spheres," *Izv. Akad. Nauk. SSR. Ser. Geofiz.*, 1963, no. 4, pp. 648–653.

[5] D. J. Angelakos and K. Kumagai, "High-frequency scattering by multiple spheres," *IEEE Trans. Antennas Propagat.*, vol. AP-13, Jan. 1964, pp. 105–109.

[6] O. Lillesaeter, "Scattering of microwaves by adjacent water droplets in air," in *Proc. World Conf. Radio Meterology*, Sept. 1964, pp. 192–193.

[7] C. Liang and Y. T. Lo, "Scattering by two spheres," *Radio Sci.*, vol. 2, 1967, no. 12, pp. 1481–1495.

[8] V. Twersky, "Multiple scattering of electromagnetic waves by arbitrary configurations," *J. Math. Phys.*, vol. 8, 1967, no. 3, pp. 589–610.

[9] R. K. Crane, "Cooperative scattering by dielectric spheres," M.I.T. Lincoln Lab., Lexington, Mass., Tech. Note 1967-31, 1967.

[10] V. Twersky, "On multiple scattering of waves," *J. Res. Nat. Bur. Stand.*, vol. 640, 1960, no. 6, pp. 715–730.

[11] J. E. Burke and V. Twersky, "On scattering of waves by many bodies," *Radio Sci.*, vol. 680, 1964, pp. 500–510.

[12] J. Bruning and Y. T. Lo, "Multiple scattering by spheres," Antenna Lab., Univ. Illinois, Urbana, Tech. Rep. 69-5, 1969.

[13] S. Stein, "Addition theorems for spherical wave functions," *Quart. Appl. Math.*, vol. 19, 1961, no. 1, pp. 15–24.

[14] O. R. Cruzan, "Translational addition theorems for spherical vector wave functions," *Quart. Appl. Math.*, vol. 20, 1962, pp. 33–40.

[15] S. Levine and G. O. Olaofe, "Scattering of electromagnetic waves by two equal spherical particles," *J. Colloid Interface Sci.*, vol. 27, 1968, pp. 442–457.

[16] J. A. Stratton, *Electromagnetic Theory*. New York: McGraw-Hill, 1941.

[17] B. R. Levy and J. B. Keller, "Diffraction by a smooth object," *Commun. Pure Appl. Math.*, vol. 12, 1959, no. 1, pp. 159–209.

[18] W. Franz, "Über die Greenschen funktionen des zylinders und der kugel," *Z. Naturforsch.*, vol. 9, 1954, pp. 705–716.

[19] T. B. A. Senior and R. F. Goodrich, "Scattering by a sphere," *Proc. Inst. Elec. Eng.*, vol. 3, 1964, pp. 907–916.

[20] J. H. Bruning and Y. T. Lo, "Electromagnetic scattering by two spheres," *Proc. IEEE* (Letters), vol. 56, Jan. 1968, pp. 119–120.

[21] R. R. Bonkowski, C. R. Lubitz, and C. E. Schensted, "Studies in radar cross-section VI:—cross-sections of corner reflectors and other multiple scatterers at microwave frequencies," Univ. Michigan, Ann Arbor, Tech. Rep. UMM-106, 1953.

[22] A. R. Edmonds, *Angular Momentum in Quantum Mechanics*. Princeton, N. J.: Princeton Univ. Press, 1957.

[23] A. L. Aden and M. Kerker, "Scattering of electromagnetic waves by two concentric spheres," *J. Appl. Phys.*, vol. 22, 1951, p. 1242.

[24] S. Levine and M. Kerker, "Scattering of electromagnetic waves from two concentric spheres, when outer shell has a variable refractive index," in *Electromagnetic Scattering*, M. Kerker, Ed. Oxford, England: Pergamon, 1963.

[25] J. H. Bruning and Y. T. Lo, "Multiple scattering of EM waves by spheres part II—numerical and experimental results," this issue, pp. 391–400.